Design and Simulation of a Resonant Converter Based EV Charger for ITUEV Team

Adnan Alhallak[1], Güven Onur[2], and Derya Ahmet Kocabas[2]

[1]Baykar Makine A.Ş., Hadımköy Istanbul, Turkey
adnan.alhallak@baykartech.com,
[2]Istanbul Technical University, Istanbul, Turkey
onurgu@itu.edu.tr, kocabasde@itu.edu.tr

Abstract

For EV battery chargers, high-power density and high-efficiency charging methods are essential. Chargers can increase the disturbance on AC power grid and an efficient charger with low distortion is needed. The power arrangement for a battery charger comprises an AC-to-DC converter featuring power factor correction (PFC), followed by an isolated DC-to-DC converter. Because of its many benefits, the LLC-type series resonant converter has become the most popular topology.
In this study, an EV charger was designed based on PFC and LLC resonant converters. The topology of the charger was investigated. The design equations of PFC and LLC resonant converters were given. Voltage loop control was implemented to the PFC converter and LLC resonant converter was controlled by a dual-loop control system. Continuous current (CC) and continuous voltage (CV) modes were implemented for safety. The completed design is served for the use of ITU Electrical Vehicle Team.

1. Introduction

Charging EV batteries needs a high power density and high efficiency charging technology and increase in battery capacities results in e need of reduced charging time [1]. A smart charger has low distortion and the capability to react to battery's state and to adjust charging operations in accordance with the battery's algorithm while basic charger maintains a consistent output without adjusting it over time or considering the battery's charge level [1].

Because the power flow is interrupted and the duty cycle is regulated interrupted in the traditional PWM method hard switching occurs in all switching devices, characterized by sudden shifts in currents and voltages, resulting in considerable noise production and switching losses. In contrast, the resonant switching method handles power in a sinusoidal manner and gently commutes the switching devices that decrease both switching losses and noise levels. [2]

By increasing the switching frequency, passive component dimensions can be reduced. [3]. Zero voltage switching (ZVS) is possible with LLC converters over their whole operating range, permitting the integration of magnetic elements into a transformer and effectively utilizing all relevant parasitic components, such as semiconductor junction capacitances [4].

An isolated DC-to-DC converter comes after an AC-to-DC converter with power factor correction (PFC) is the arrangement of the battery charger circuit [2]. Throughout the battery charging process, this design effectively eradicates current ripples at both low and high frequencies, all without the need for a large filter capacitor. Instead, it employs a high-frequency transformer, which not only maintains battery life but also avoids increasing the charger's size.

A traditional continuous conduction mode (CCM) boost topology, as illustrated in Figure 1, is employed by the AC-to-DC power factor correction (PFC) converter. [5]. An LLC resonant converter is chosen for its exceptional efficiency, minimal electromagnetic interference (EMI) output, extensive operational capacity, and capacity to achieve high power density [1]. Besides, EV charger contains an electromagnetic interference (EMI) filter [4].

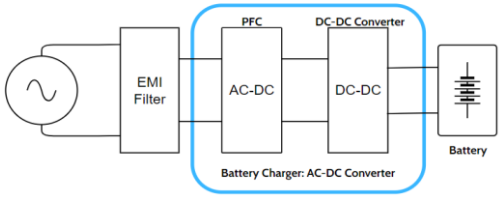

Fig. 1. A battery charger's standard power structure.

DC-DC converters are widely utilized across various applications, with a primary focus on achieving both high efficiency and high power density. By operating at higher switching frequencies and maintaining elevated efficiency, resonant converters meet these requirements [6]. Comparing the LLC resonant converter to series and parallel resonant converters, the latter has a smaller switching band variation and a larger output voltage range, allowing for more output regulation [7, 8].

In this study, a PFC and LLC resonant converter based EV charger was designed. In section 2, mathematical background is given. Voltage loop control was implemented to the PFC converter and LLC resonant converter was controlled by a dual-loop control system. For a safe operation CC-CV control were implemented. Operational limits, simulation model and results are all presented in Section 3. The completed design is served for the use of ITU Electrical Vehicle Team.

2. General Information

Power factor correction (PFC) is used in the AC-DC section to improve the input power factor, and frequency control is used in the DC-DC stage to operate a full-bridge LLC resonant converter with galvanic isolation. Taking into account cost, dependability, and effectiveness, the LLC resonant converter stands as the appropriate choice for electric vehicle (EV) battery systems [1].

The boost PFC circuit operating in continuous conduction mode (CCM) is without a doubt the most popular option for medium- and high-power applications. Figure 2 illustrates the fundamental architecture of the boost converter, which uses a variety of specialized control techniques to produce low-distorted input currents and a power factor of nearly unity [7].

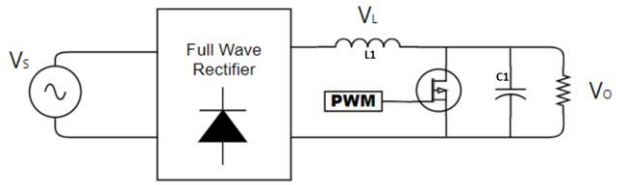

Fig. 2. Single-phase PFC boost converter.

Fig. 3 illustrates how the system's current harmonic distortion is reduced during this phase after the input voltage has been rectified. A constant voltage and current are fed to the LLC converter to optimize the output's power density and efficiency. The leakage inductor reflected in the primary side is represented by Lr, the magnetizing inductor by Lm, and the resonant capacitor by Cr. S1 and S4, as well as S2 and S3, are grouped in the switch network. In order to generate a balanced square waveform having amplitude of Vin, each group is alternated with a 50% duty cycle at a frequency of fs, and there is a 180° phase difference between the groups. This symmetrical square pulse is sent to the resonant tank, which is connected to the load by a desired transformer, to transfer energy to the load. [8]

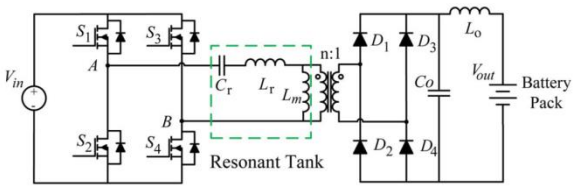

Fig. 3. LLC resonant full-bridge converter [7].

The process of designing the resonant network varies when applied to battery charging scenarios. Typically, the lithium-ion battery charging procedure comprises two primary phases. Fig. 4 illustrates an initial constant-current (CC) charging stage and a subsequent constant-voltage (CV) charging stage.

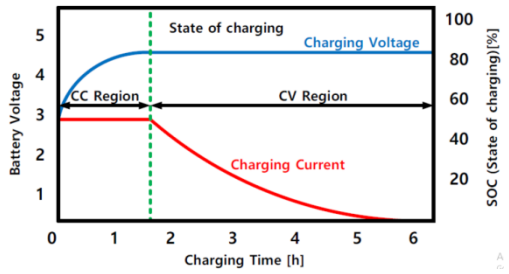

Fig. 4. The profile of the CC-CV mode graph [9].

A comprehensive examination of LLC resonant converters is essential for ensuring reliability. However, due to the intricate nature of the model, it is not straightforward to derive a practical design approach from it. Approaches utilizing FHA (Frequency Domain Harmonic Analysis) analysis are comparatively easier to handle, particularly when the resonant tank circuit is at or above its resonance frequency. Reverse recovery losses in the output rectifier diodes are greater than in the frequency range below resonance because the zero-current switching (ZCS) capabilities of the diodes are lost above resonance frequency. In the below-resonance region, the FHA is still relevant but less precise [8].

The primary objective when selecting the components for the resonant tank circuit is to ensure that ZVS on the primary side is maintained across the entire load range, from zero to full load. Since this load-insensitive point is situated within the zero-voltage switching (ZVS) zone, the optimal decision for ensuring a stable output voltage under different load conditions is to configure the converter to function at its resonant frequency when the input voltage is at its nominal value. [8]. To achieve the highest efficiency, it is necessary to operate in the vicinity of frequencies where the impedance of the resonant tank is extremely low. Furthermore, to ensure ZVS and avoid ZCS within Region 3, it is necessary to operate within Region 2, as shown in Fig. 5 [1].

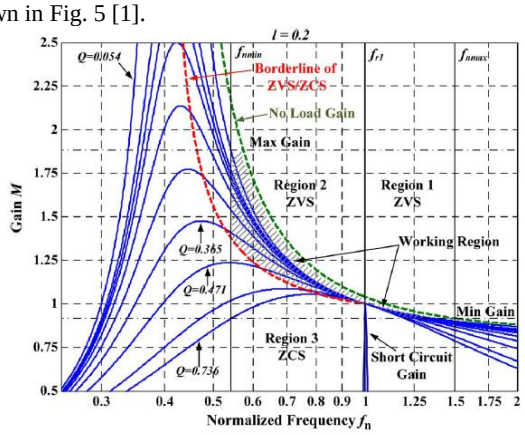

Fig. 5. The DC amplification properties of the LLC resonant converter utilizing FHA [7].

2.1. Mathematical Design

The converter could operate at frequencies where the resonance of the junction capacitances of the rectifier diodes and other parasitic elements within the circuit occurs, leading to an undesirable increase in the output voltage if the method of limiting the maximum switching frequency isn't applied [1],[10]. Therefore, it is advisable to cap the maximum switching frequency at a range of 2 to 2.5 times the resonant frequency [1], [7]. Lowering the k or Q values might result in a greater peak gain. When k or Q is reduced for a given resonant frequency (f_{r1}), the magnetizing inductance is reduced, resulting in higher circulating current [4].

DC voltage gain parameters are quality factor (Q), inductance ratio (k) and transformer ratio (a) as given in (1-3).

$$Q = \frac{1}{R_{ac}}\sqrt{\frac{L_r}{C_r}} \quad (1)$$

$$k = \frac{L_m}{L_r} \quad (2)$$

$$a = \frac{V_{in\,min}}{2(V_o + V_F)} \quad (3)$$

$$G_v = \frac{2\,a\,V_o}{V_{in}} \quad (4)$$

$$G_v = \frac{\left(\frac{\omega^2}{\omega_{r2}^2}\right)\left(\frac{k}{k+1}\right)}{j\left(\frac{\omega}{\omega_{r1}}\right)\left(1-\frac{\omega^2}{\omega_{r1}^2}\right)Q\frac{(k+1)^2}{2k+1}+(1-\frac{\omega^2}{\omega_{r2}^2})} \quad (5)$$

$$R_{ac} = \frac{8}{\pi^2}a^2 R_L \quad (6)$$

Resonance frequencies are as below.

$$f_{r1} = \frac{1}{2\pi\sqrt{(L_r C_r)}} \quad (7)$$

$$f_{r2} = \frac{1}{2\pi\sqrt{(L_r+L_m)C_r}} \quad (8)$$

whatever the input and output voltage ratings, the LLC resonant converter efficiently sends zero power to its output within a certain frequency range. This region is referred to as the cutoff region, and the corresponding frequency is termed the cutoff frequency [11]. V_F represents the approximated voltage decrease across every one of the secondary rectifiers.

$$f_{co} = \frac{\pi}{2}\sqrt{\frac{1}{1+k}} \times \frac{1}{\cos^{-1}\left(\frac{k}{2\,a\,M\,(1+k)}\right)} \times f_{r1} \quad (9)$$

$$M = \frac{V_o+V_F}{V_{in}} \quad (10)$$

During cutoff mode, the depicted value of the tank current's peak is as follows:

$$I_{mco} = \frac{V_{in_{max}}}{4\,\pi\,f_{r1}\,L_m}\sqrt{\left(4\,(1+k)\,a^2\,M_{min}^2 - \frac{k^2}{1+k}\right)} \quad (11)$$

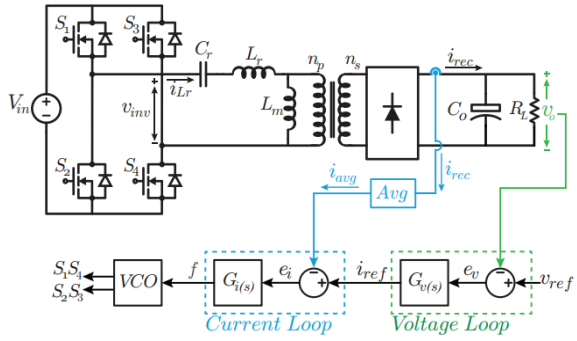

Fig. 6. Circuit design of the proposed dual-loop controller [12]

EV charging systems frequently employ CC-CV mode algorithms. CV denotes a technique for regulating and maintaining a stable output voltage that is supplied to the battery. CC mode, in contrast to CV mode, regulates a consistent current throughout the entire charging cycle, from the beginning to the end. It's crucial to manage the charging current and duration effectively to avoid overcharging, which can harm the battery. Charging commences in CC mode from starting point, allowing it to rapidly reach an SOC of 80 to 90%. When the SOC reaches 80%, CC mode is deactivated, and CV mode takes over as Fig. 4. A dual-loop control system with an outer voltage loop and an inner current loop is suggested for the LLC resonant converter, and it is shown in Fig. 6. The LLC converter exhibits distinct dynamic behavior based on its operational states, which comprise of states below resonance, at resonance, and above resonance. When the switching frequency is smaller than the resonant frequency, an easy-to-understand equivalent circuit model is created by simplifying the extended descriptive function method and adding significant modifications specific to this situation [13].

2.2. Designed Charger

Within this system, the PFC circuit serves the dual purpose of power factor correction and voltage stabilization for the subsequent DC/DC stage. To design the PFC converter the input parameters are as in Table 1.

Table 1. PFC converter Design Specifications

Parameter	Value
Input Voltage (V_{in})	220 V AC
Rated output power (P_o)	500 W
Line frequency	50 Hz
Output DC voltage (V_o)	370 V DC
Switching frequency (f_{sw})	100 kHz
Efficiency (η)	98%

Based on Table 1 a duty cycle between 0.11 and 0.22 has been determined. By using these values at 100 kHz an inductance of 1053 μH and an output capacitor of 411.253 μF was calculated, but the capacitor is chosen to be 600 μF.

LLC converter was designed to have a higher efficiency and power density and lower EMI for the information in Table 2.

Table 2. LLC Resonant converter Design Specifications

Parameters	Value
Input Voltage Range	350 – 400 V DC
Input Voltage Nominal	370 V DC
Output Voltage Range	80 – 100 V DC
Output Current	5 A
Max Output Power	500 W
Resonant Frequency f_{r1}	80 KHz
Max Switching Frequency f_s	180 KHz
Efficiency (η)	98%
Parasitic Capacitance of Node HB (C_{HB})	400 ρF
Dead Time of Driver Circuit (T_d)	400 ns
Quality Factor (Q)	0.59
Parallel-to-series inductance ratio (k)	9.32

By using the mathematical method, main parameters were calculated as in Table 3.

Table 3. LLC resonant tank parameters and operating conditions

Parameter	Symbol	Value
Parallel resonant inductance	L_m	604.2 μH
Series resonant inductance	L_r	64.774 μH
Resonant capacitance	C_r	61.102 nF
Minimum switching frequency	$f_{s_{min}}$	64.956 kHz
Switched current	I_s	0.9568 A
Tank current phase angle	θ_1	24.63 Deg

The control loop system was designed and coefficients for CC and CV regions to operate effectively in both. All system components were built in MATLAB Simulink as in Fig. 7.

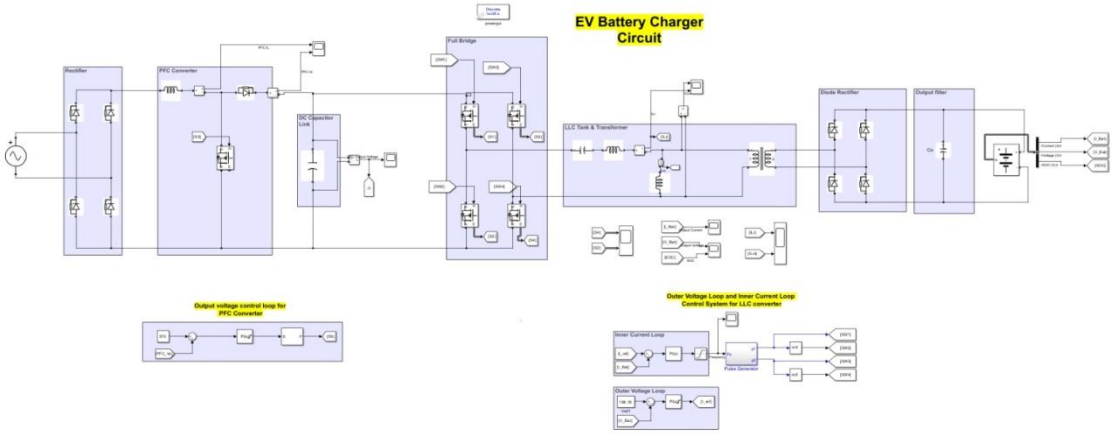

Fig 7. Design of EV battery charger circuit in MATLAB Simulink.

3. Simulations

Numerous simulations were conducted by employing an open PID Tuner by generating input references with different frequencies to observe the system response. The CC region current was 5 A and CV region voltage was 108 V.

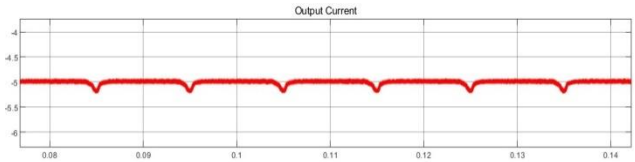

Fig 8. Waveform of output current.

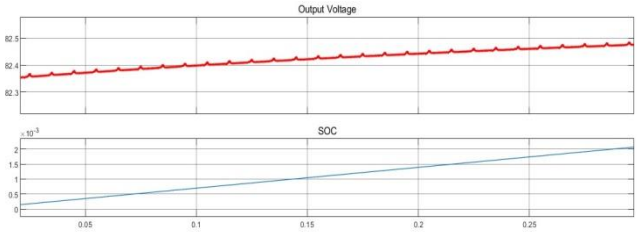

Fig 9. Waveform of output voltage and SOC.

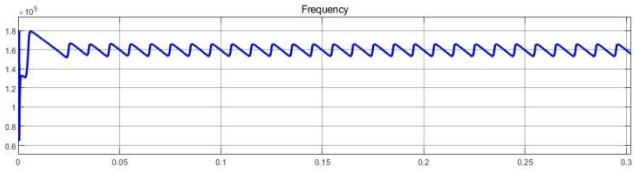

Fig 10. Waveform of switching frequency.

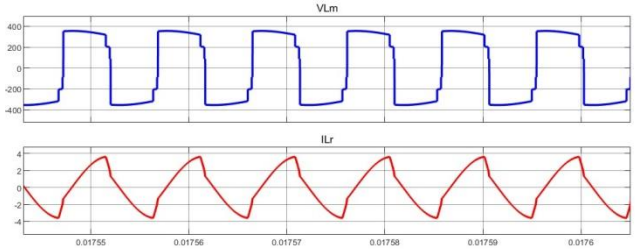

Fig 11. Primary voltage of transformer and the current of series inductor L_r.

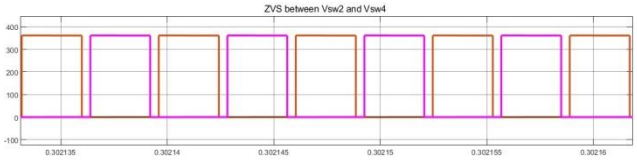

Fig 12. Voltages of SW2 and SW4 and ZVS mode.

First, the circuit model was initiated for zero SOC and the changes between Fig. 8-12 were obtained. It was seen that current was successfully held at -5 A as in Fig. 8, while SOC was rising as in Fig. 9, proving the operation in CC region. The Switch voltages are represented in Fig. 12.

For an initial SOC of 80%, the simulation results are given in Fig. 13-15. The voltage of the battery was settled to 108.15 V limit, proving that the charger was in CV mode control. The output current was managed to be held at -4.65 A. Output voltage was settled around 108.15 V.

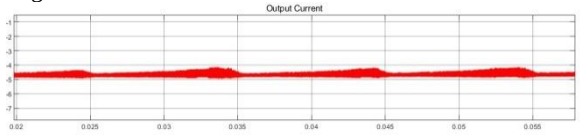

Fig 13. Waveform of output current at SOC 80%.

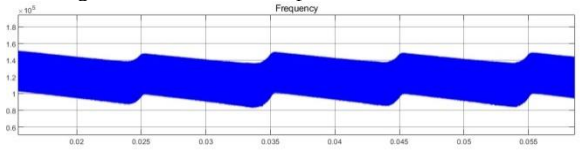

Fig 14. Waveform of switching frequency of 80% SOC.

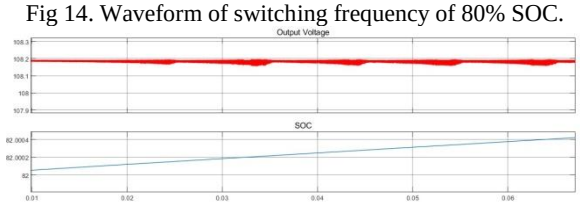

Fig 15. Waveform of output voltage and SOC at 80% SOC.

After SOC increased above 80% the current began to decrease gradually until it reaches to 0A when the SOC reaches 100%. When SOC reached to 98%, the current fell under 0.5A and the voltage stayed constant at 108.15V, while the controller makes the charger circuit works in maximum switching frequency. All changes for the last operation can be seen in Fig. 16 to Fig. 18.

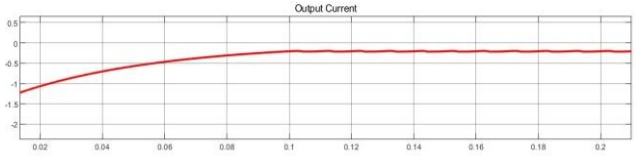

Fig 16. Waveform of output current at 98% SOC.

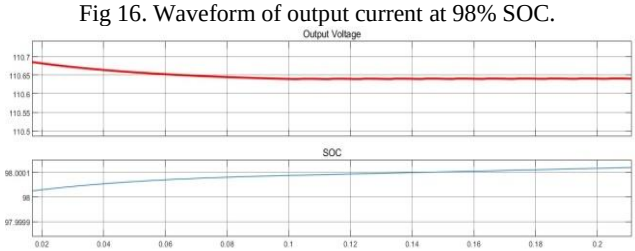

Fig 17. Waveform of output voltage and SOC at 98% SOC.

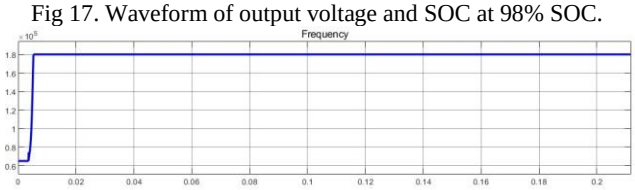

Fig 18. Waveform of switching frequency at 98% SOC.

It can be seen form the results that as SOC got closer to 100%, the current got closer to 0A, and the charger entered floating charging mode not to overcharge the battery.

6. Conclusions

An EV charger system accommodating both PFC and LLC resonant converter stages was designed and mathematical model is presented. The design was connected to a rated voltage of 370 V DC bar and aims to charge a 100 V battery. Design specifications are all given. A model indicating CC and CV control was built in MATLAB. A load scenario was operated beginning from zero up-to 100% SOC. It was seen that charging current kept constant up-to 80% SOC and the charger shifted to CV voltage mode with a decreasing charge current as SOC increases. As the SOC value reached to 100%, charging current slightly fell down to zero gradually.

All-in-all, a numerical design and simulation of an EV charger with a successful CC-CV control application was achieved and served to the use of ITU Electrical Vehicle Team.

7. References

[1] Musavi, Fariborz et al. “An LLC Resonant DC–DC Converter for Wide Output Voltage Range Battery Charging Applications.” IEEE Transactions on Power Electronics 28 (2013): 5437-5445.

[2] Steigerwald, Robert. “A comparison of half-bridge resonant converter topologies.” 1987 IEEE Applied Power Electronics conference and Exposition (1987): 135-144.

[3] A. F. Witulski and R. W. Erickson, "Design of the Series Resonant Converter for Minimum Component Stress," in IEEE Transactions on Aerospace and Electronic Systems, vol. AES-22, no. 4, pp. 356-363, July 1986, doi: 10.1109/TAES.1986.310771.

[4] H. Choi, "Analysis and Design of LLC Resonant Converter with Integrated Transformer," APEC 07 - Twenty-Second Annual IEEE Applied Power Electronics Conference and Exposition, 2007, pp. 1630-1635, doi: 10.1109/APEX.2007.357736.

[5] Liyu Yang et al., "Modeling and characterization of a 1 KW CCM PFC converter for conducted EMI prediction," Nineteenth Annual IEEE Applied Power Electronics Conference and Exposition, 2004. APEC '04., Anaheim, CA, USA, 2004, pp. 763-769 vol.2, doi: 10.1109/APEC.2004.1295909.

[6] B. Lu, W. Liu, Y. Liang, F. C. Lee, and J. D. van Wyk, Optimal design methodology for LLC resonant converter," in Twenty-First Annual IEEE Applied Power Electronics Conference and Exposition, 2006. APEC '06., March 2006, pp. 6 pp. pp.533-538, doi: 10.1109/APEC.2006.1620590.

[7] Beiranvand, Reza & Rashidian, Bizhan & Zolghadri, M.R. & Alavi, Mohammad. (2012). A Design Procedure for Optimizing the LLC Resonant Converter as a Wide Output Range Voltage Source. Power Electronics, IEEE Transactions on. 27. 3749-3763.

[8] D. Czarkowski and M. K. Kazimierczuk, "Phase-controlled CLL resonant converter," Proceedings Eighth Annual Applied Power Electronics Conference and Exposition, 1993, pp. 432-438, doi: 10.1109/APEC.1993.290696.

[7] Figueiredo, Joao Paulo M. et al. “A review of single-phase PFC topologies based on the boost converter.” 2010 9th IEEE/IAS International Conference on Industry Applications - INDUSCON 2010 (2010): 1-6.

[8] Deng, Junjun & Li, Siqi & Hu, Sideng & Mi, Chris & Ma, Ruiqing. (2014). Design Methodology of LLC Resonant Converters for Electric Vehicle Battery Chargers. Vehicular Technology, IEEE Transactions on. 63. 1581-1592.

[9] Kim, Do-Hyun & Kim, Min-Soo & Nengroo, Sarvar & Kim, Chang-Hee & Kim, Hee-Je. (2019). LLC Resonant Converter for LEV (Light Electric Vehicle) Fast Chargers. Electronics. 8, 362. 10.3390/electronics8030362.

[10] B. Lee, M. Kim, C. Kim, K. Park and G. Moon, "Analysis of LLC Resonant Converter considering effects of parasitic components," INTELEC 2009 - 31st International Telecommunications Energy Conference, 2009, pp. 1-6, doi: 10.1109/INTLEC.2009.5351740

[11] Adragna, C., De Simone, S., & Spini, C. (2008). A design methodology for LLC resonant converters based on inspection of resonant tank currents. 2008 Twenty-Third Annual IEEE Applied Power Electronics Conference and Exposition, 1361-1367.

[12] Degioanni, F., Zurbriggen, I.G., & Ordonez, M. (2018). Dual-Loop Controller for LLC Resonant Converters Using an Average Equivalent Model. IEEE Transactions on Power Electronics, 33, 9875-9889.

[13] Lordoglu, Abdulsamed & Gulbahce, Mehmet & Kocabas, Derya & Dusmez, Serkan. (2021). Extended Describing Function Modeling and Closed-Loop Control of LLC Converter in Battery Charging Applications. 274-279. 10.1109/OPTIM-ACEMP50812.2021.9590032.